ELSEVIER

Polymer 42 (2001) 7181–7195

polymer

www.elsevier.nl/locate/polymer

Morphology and crystal structure of CTFMP and bulk polymerized poly(trimethylene terephthalate)

J. Yang[a], G. Sidoti[a], J. Liu[a], P.H. Geil[a,*], C.Y. Li[b], S.Z. D. Cheng[b]

[a]Department of Materials Science and Engineering, University of Illinois, 1304 W. Green Street, Urbana, IL 61801, USA
[b]Department of Polymer Science, The University of Akron, Akron, OH 44325, USA

Received 2 September 2000; received in revised form 15 October 2000; accepted 20 October 2000

Abstract

Poly(trimethylene terephthalate) (PTT) has been polymerized at temperatures between 150 and 220°C as extended chain lamellar single crystals, ca 100 Å thick, by the confined thin film melt polymerization (CTFMP) technique. The crystal structure, determined from electron diffraction patterns and modeling using the CERIUS^2 simulation program is compared with that of solution grown crystals from higher molecular weight commercial PTT and PTT polymerized in the bulk at temperatures from 180 to 220°C; the crystal density is highest for the CTFMP material and least for the solution precipitated commercial PTT. The triclinic unit cell of PTT contains two chemical repeat units from a single chain, with lattice parameters of $a = 4.53$, $b = 6.15$, $c = 18.61$ Å, $\alpha = 97°$, $\beta = 92°$, $\gamma = 111°$, $\rho = 1.448$ g/cm^3. © 2001 Elsevier Science Ltd. All rights reserved.

Keywords: Poly(trimethylene terephthalate); Confined thin film melt polymerization; Crystal structure

1. Introduction

With the development of economical methods for the production of 1,3-propanediol, there has been increased commercial interest in the production and utilization, primarily as carpet yarn, of poly(trimethylene terephthalate) (PTT) [1]. Having recently characterized the crystal structure of several other polyesters, including poly(ethylene terephthalate) (PET) [2], poly(butylene terephthalate) (PBT) (α-form) [3] and poly(ethylene naphthalate) (PEN) [4] using electron diffraction from single crystals and computer modeling, we describe here a similar study of PTT. The single crystals and, for PTT spherulites, were grown by our confined thin film melt polymerization (CTFMP) technique [5], with the computer modeling and diffraction pattern simulation being done using CERIUS^2 [6]. The results for the nascent crystals are compared with literature values primarily based on X-ray patterns from fibers. In the summary by Hall [7], the "best" unit cell for PTT is listed as triclinic; $a = 4.60$, $b = 6.22$ and $c = 18.36$ Å; $\alpha = 97.8°$, $\beta = 90.2°$ and $\gamma = 111.3°$; $\rho = 1.414$ g/cm^3; $T_m = 228$°C. More recently Wang et al. [8] used X-ray diffraction from a sample crystallized isothermally from the melt at 150°C to essentially confirm these unit cell parameters (see Table 2).

For PET, the crystal structure (and crystal density appears to be a function of processing history (see Table 1 in Ref. [2]). Our results for the nascent crystal structure yielded a higher density than that obtained for any processing history. PBT and PEN are polymorphic, the crystal phase again depending on processing history. The ED results for the α-form of PBT, the phase found in relaxed PBT fibers or samples crystallized without strain, were similar to those reported in the literature (see Table 1 in Ref. [3]). For PEN, ED patterns were obtained from three phases using both CTFMP samples and samples crystallized isothermally from the melt. The spacings and angles for the triclinic α-form patterns, only obtained, infrequently, from isothermally crystallized samples, agreed well with those reported by Mencik [9] for samples crystallized from the glass by annealing or from the melt at low temperatures (<200°C). It is also found in fibers, along with a β-form, the amount of β-increasing with fiber take-up speed (i.e. orientation) [10]. ED patterns from the β-phase were obtained from both isothermally crystallized melt samples (hedrites) and some regions of CTFMP samples. CERIUS^2 modeling of this phase resulted in a different unit cell than that reported in the literature (monoclinic rather than triclinic, [10]), but with strong reflections

---

* Corresponding author. Tel.: +1-217-333-0149; fax: +1-217-333-2736.
E-mail address: geil@uiuc.edu (P.H. Geil).

0032-3861/01/$ - see front matter © 2001 Elsevier Science Ltd. All rights reserved.
PII: S0032-3861(01)00044-1

at similar 2θ diffraction angles. The single crystal CTFMP samples and spherulites in the high-temperature melt crystallized samples yielded ED patterns from a third phase, labeled γ, whose crystal structure was not determined [4].

Our interests here include comparison of the unit cell parameters of nascent CTFMP PTT with that obtained from fibers and solution grown, folded chain, single crystals [11] and the morphology of the CTFMP samples in comparison with those of PET and PBT. Only limited studies were made of CTFMP PEN, single crystal lamellae grown by melt crystallization of pre-formed polymer being used for most of the diffraction studies.

2. Experimental

Dilute (ca. 1%), fresh acetone solutions of terephthaloyl chloride ($T_m = 80°C$) or dimethyl terephthalate (DMT, $T_m = 140°C$) and 1,3-propanediol (PDO, a liquid at room temperature with $T_b = 214°C$) (all from Aldrich Chemical Co., Inc., Milwaukee, WI, and used as purchased) were cast on glass cover slips or mica and dried. Two of these coated slips were combined with the films face to face, wrapped in aluminum foil and heated at various temperatures (T_ps) between 150 and 240°C (i.e. both below and above the T_m of high molecular weight PTT) and times (t_ps) on a thermostated hot plate. Polymerization at low T_p resulted in formation of poly(terephthalic anhydride) (PTA) [12]. Following polymerization, the resulting sandwiched slips were separated and washed several times with acetone. The dried thin film samples were shadowed with Pt–C for image observations or coated with carbon and Au for ED spacing calibrations. The lamellar crystals on the slips can be separated from the substrate glass either by stripping with poly(acrylic acid) or floated off on the surface of HF solution. After washing in water these thin film samples were picked up on transmission electron microscope (TEM) grids. Standard transmission microscopy (STM) preparation techniques were used (Pt/C shadowing, Au decoration for ED calibration), with removal from the substrate by floating on dilute HF or dissolution of the substrate on more concentrated HF. After washing in water, these thin film samples were picked up on TEM grids.

Bulk polymerized DMT/PDO (180°C/24 h, 180°C/72 h, 200°C/72 h, 210°C/72 h and 220°C/72 h, under N_2) were used for differential scanning calorimetry (DSC, DuPont DSC-10, Wilmington, DE), scan rate of 20°C/min) and Fourier transform infrared spectroscopy (FTIR, Galaxy 5000, ATI Mattson, Madison, WI) using KBr pellets, 32 scans at 4 cm^{-1} resolution). They were also used for wide angle (WAXD) and small angle (SAXD) X-ray diffraction. on a Siemens (Bruker AXS, Madison, WI) M18HF22 Rotating Anode power supply with a 0.3×3 mm^2 filament and Cu target operated at 80 mA, 40 kV. WAXD patterns were taken using a Siemens GADDS system with a Siemens HiStar 2D position sensitive detector. For SAXD, a Siemens Anton Parr small angle camera was used, along with a 2D position sensitive detector. Peaks were calculated and spacings were determined using the Siemens software. X-ray fiber patterns were obtained from DuPont fibers supplied by B. Hsaio. For WAXD, SAXD, DSC and IR measurements of the DuPont PTT sample, the fibers were dissolved in nitrobenzene at 200°C, cooled under ambient conditions (precipitated), filtered and dried.

Polymer from the fibers was also used for preparing solution-grown single crystals by isothermal crystallization at 136°C for 48 h in nitrobenzene following a simplified version of the directions of Poulin-Dandurand et al. [11] The fibers were dissolved at 0.05 wt.% concentration at 170°C, filtered hot and the solute then cooled to 136°C for crystallization. These crystals were prepared for TEM and ED as above, following drying of the suspension on C-coated glass microscope slides. TEM and ED investigations were conducted with a Philips CM-12 (FEI Company, Hillsboro, OR) at 120 kV. In addition to [001] ED patterns, other zonal patterns were obtained by tilting the grids, permitting observation of many *hkl* reflections. In situ calibration of the ED spacings was carried out using the Au-coated samples. ED patterns were scanned with a Relisys (Milipas, CA) 9624 scanner and Adobe Photoshop software at a resolution of 1500 dpi for accuracy; the spacings were measured with the NIH Image software.

The unit cell parameters were determined by refinement using measured values of the spacings, for the ED and X-ray patterns individually, and literature values for the parameters for those not directly measured; a program supplied by A. Zhang was used [13]. The crystal structures of PTT and its chain conformation in the lattice were modeled, based on the resulting parameters for the ED data, using the CERIUS^2 (4.0) (Molecular Simulations, Inc. San Diego, CA) software with the Dreiding force field for an infinitely periodic system. The intramolecular interactions utilized (valence terms) include bond stretching, angle bending, torsional and inversion terms. The torsion angle energy was adjusted to give the best agreement between calculated and observed ED patterns. The intermolecular interactions include van der Waals and Coulomb terms. For our periodic system, the Ewald summation method was used in the minimizing calculations. Van der Waals interaction between atoms separated by three bonds is excluded from the energy term. Other parameters were usually chosen as the default options except in those cases in which settings were recommended in the manual for polymer-type periodic systems. A minimized chemical repeat unit of a single molecule was used to build the unit cell. For the simulated electron and X-ray diffraction patterns, a global isotropic temperature factor of 5 Biso ($Å^2$) was used in the calculations.

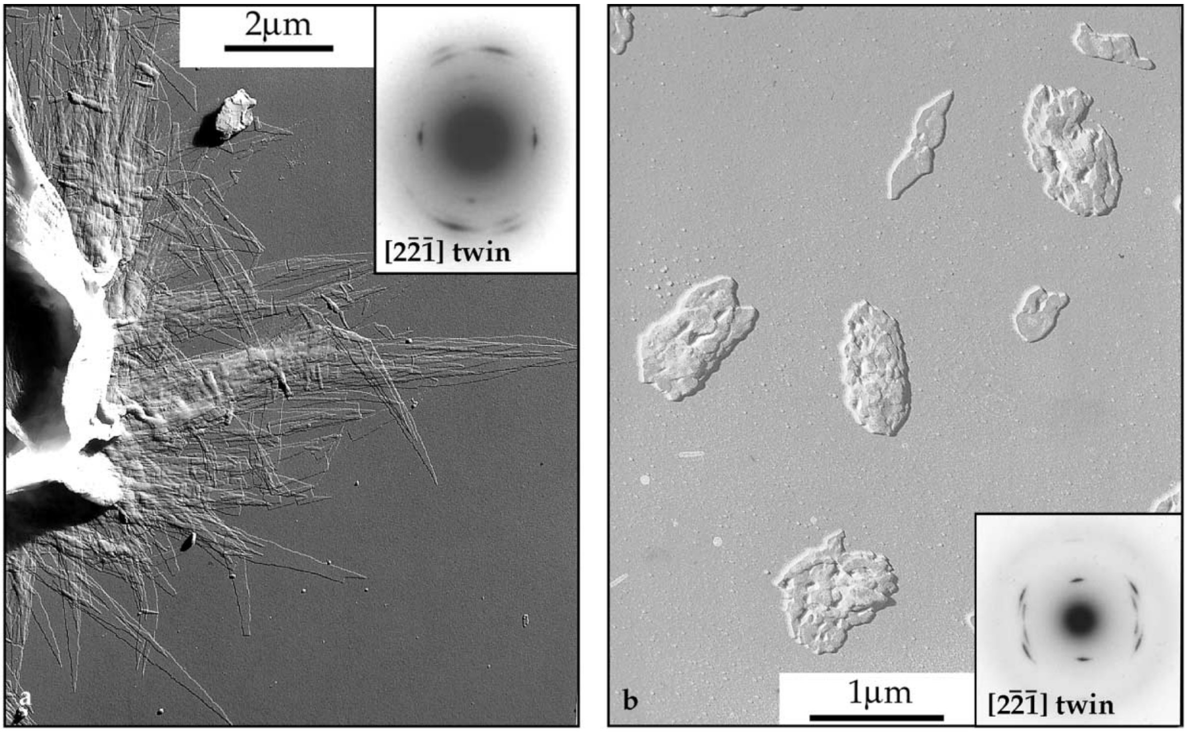

Fig. 1. PTT crystallized from nitrobenzene, crystallized isothermally at 136°C for 48 h. Both types of crystals gave rise to $[2\bar{2}\bar{1}]$ ED patterns, with those in both *a* and *b* being twinned. For both types of crystals, b^* is parallel to the long axis of the crystals.

3. Results and discussion

3.1. Morphology

Two different morphologies were observed for the solution-crystallized samples (Fig. 1) both giving rise to similar twinned $[2\bar{2}\bar{1}]$ ED patterns. Enlarged views of the ED patterns and their simulations, using CERIUS^2, are given below (Fig. 14), with reflections labeled on the simulations. Neither of these samples look identical to those of Poulin-Dandurand et al. [11] but it is possible the crystal they show (Fig. 2 in Ref. [11]) is part of one of the "fronds" in Fig. 1a. However, they obtained [001] patterns from their samples and a^* was parallel to the long axis whereas in both of our types of crystals b^* was parallel to the long axis. At present, we have no explanation for the differences in morphology observed for apparently identical crystallization conditions. The lamellae in Fig. 1a are 60–70 Å thick, while the single layer lamellae in Fig. 1b are 120–130 Å thick. In both the crystals shown in Fig. 1 b^* lies in a plane parallel to the long axis of the crystals, but at a 34° angle to the substrate.

As indicated above, attempts to prepare single crystals by CTFMP using TCl and PDO at low T_p, presumably due to the high reactivity of TCl, lead to the growth of PTA (Fig. 2a). It could be easily distinguished from PTT both by the shape of the crystals and the single chain [001] ED patterns, which involve no forbidden reflections (inset). Using DMT with PDO, however, for similar polymerization conditions (150°C/12 h), did lead to the growth of large, thin (100–110 Å) single crystals yielding somewhat tilted, twinned $[20\bar{1}]$ patterns (Fig. 2b and inset).

At 180°C, it was possible to prepare lamellar PTT single crystals by CTFMP from TCl and PDO (Fig. 3, with two magnifications); the lamellar thickness is 85–100 Å, the crystals having rough growth faces on the narrow faces of the crystals. The long faces are asymmetric, one face being smoother than the other. The ED pattern (inset at the correct angle) indicate b^* is parallel to the long axis and the substrate. The crystals rather closely resemble those grown for PET at 200°C (Fig. 1b, Ref. [2]); they, however, gave rise to [001] ED patterns whereas these crystals gave $[20\bar{1}]$ patterns. In thicker films of both TCl/PDO and DMT/PDO polymerized at this temperature, stacks of lamellae formed between the substrates, which split apart when the substrates were separated (Fig. 4a and b). Both samples gave rise to $[20\bar{1}]$ patterns as shown by the insets.

Spherulites, as well as single crystals, developed during the CTFMP process, the spherulites developing in thicker regions of the film. A series of micrographs taken during heating a DMT/PDO film to 195°C, followed by isothermal polymerization at that temperature, are shown in Fig. 5. With the PDO being liquid at room temperature and DMT melting at 140°C, the birefringent structures in Fig. 5b and subsequently must be polymer. After 270 min from the start of heating, they take on a clear spherulitic appearance, growing radially with time. An electron micrograph of possibly related structures is shown in Fig. 6, for a TCl/PDO 210°C/7 h sample grown on glass from a film that

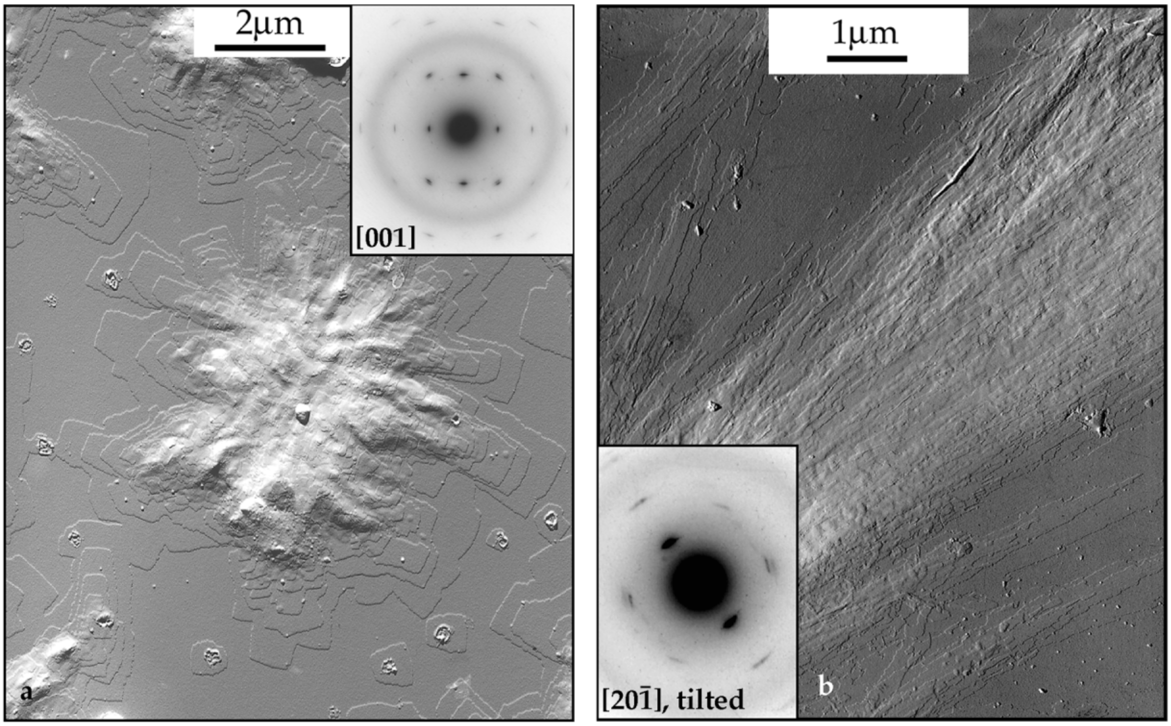

Fig. 2. (a) PTA grown by CTFMP from TCl/PDO at 155°C/6 h. The crystals are readily recognizable, essentially square ended lathes, with a one chain, rectangular ED pattern. (b) PTT grown by CTFMP from DMT/PDO at 150°C/12 h. a^* is parallel to the long axis of the elongated crystals.

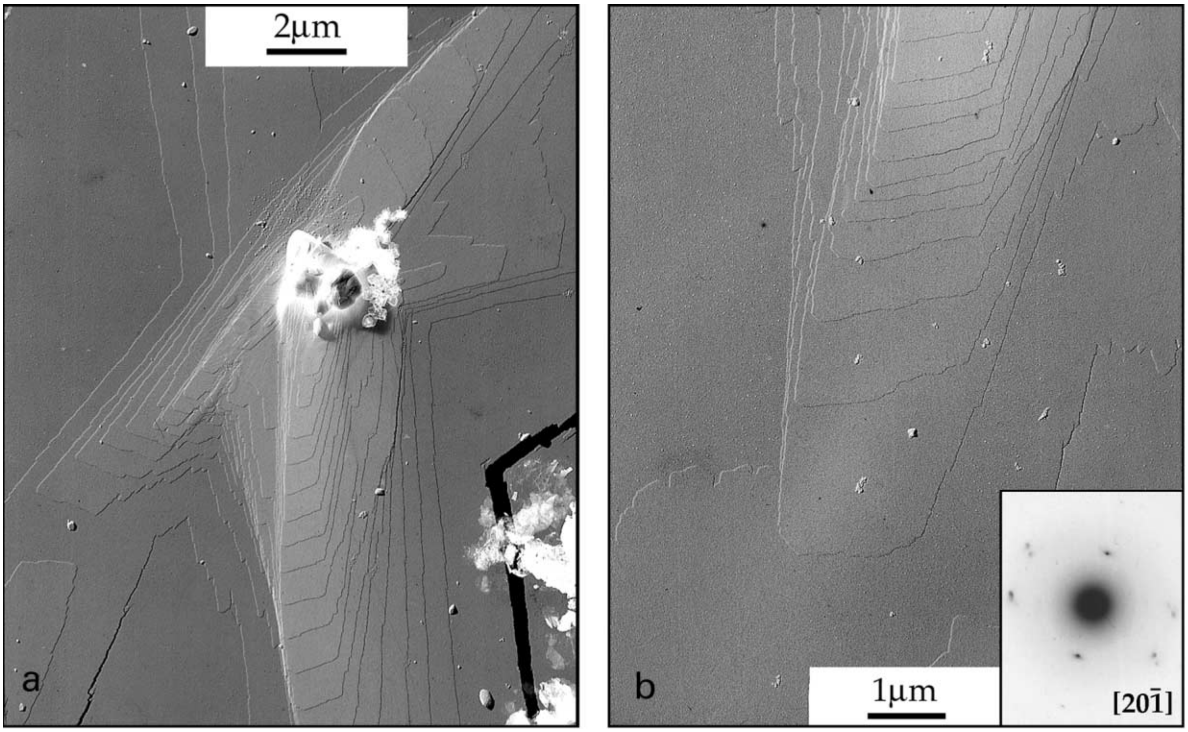

Fig. 3. (a) Single crystals of PTT from TCl/PDO, prepared at 180°C/24 h by CTFMP between glass; (b) is a higher magnification photo of the ends of the lath shaped lamellae, with the ED inserted at the proper orientation in (b).

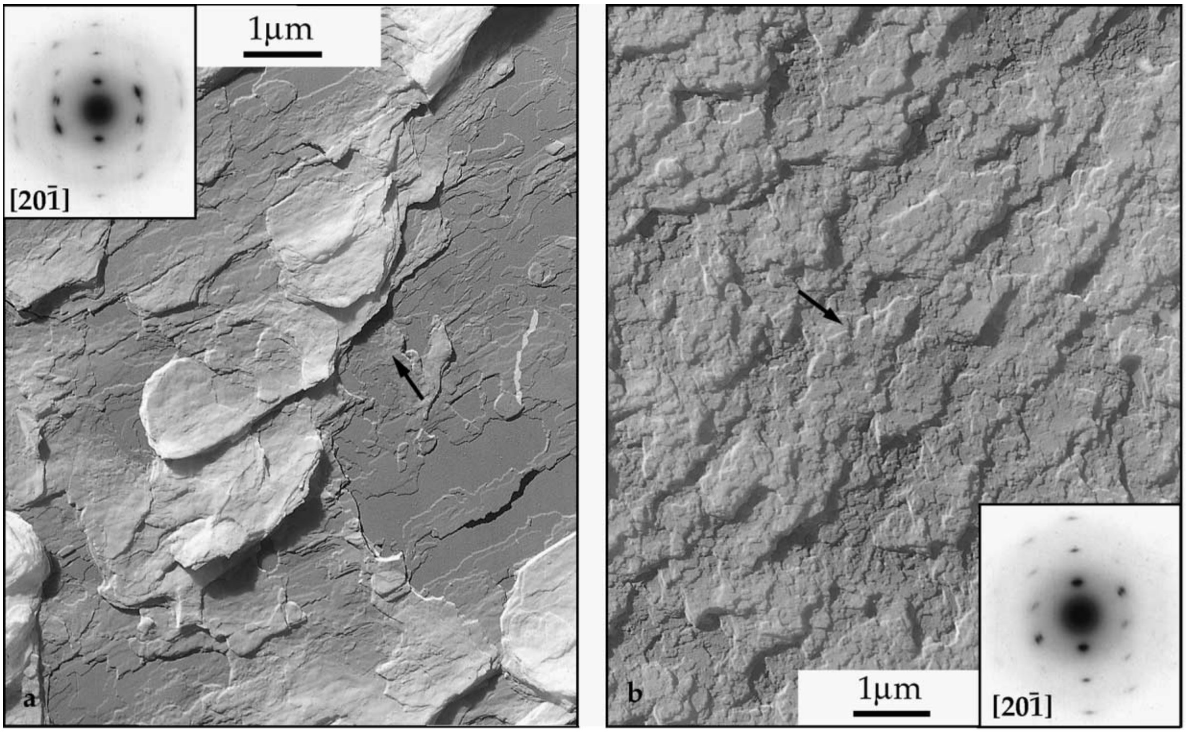

Fig. 4. Split, “thick” films of: (a) CTFMP TCl/PDO and (b) DMT/PDO polymerized at 180°C/24 h between glass. The ED patterns are inset at the correct orientation, the arrows indicating the location used for the ED patterns.

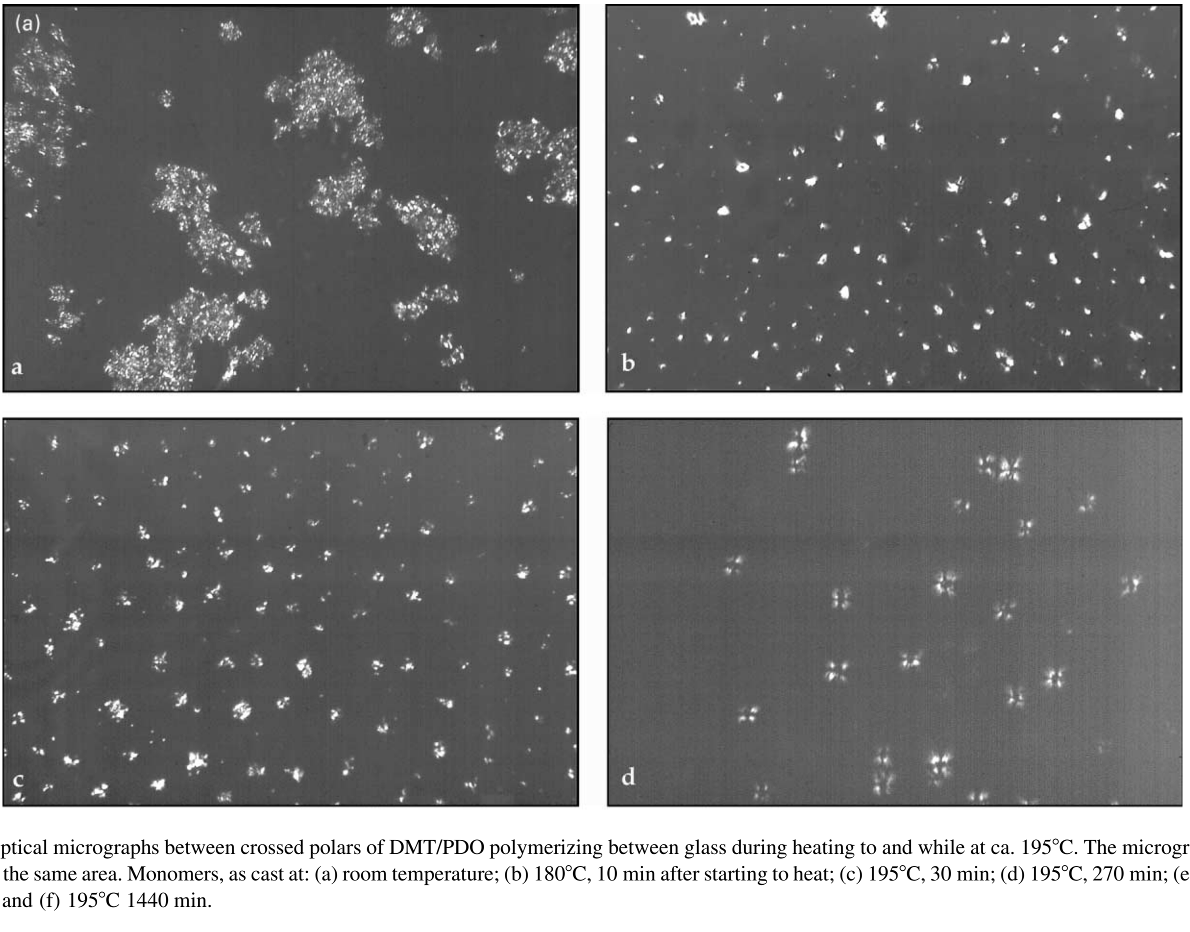

Fig. 5. Optical micrographs between crossed polars of DMT/PDO polymerizing between glass during heating to and while at ca. 195°C. The micrographs are not from the same area. Monomers, as cast at: (a) room temperature; (b) 180°C, 10 min after starting to heat; (c) 195°C, 30 min; (d) 195°C, 270 min; (e) 195°C, 720 min and (f) 195°C 1440 min.

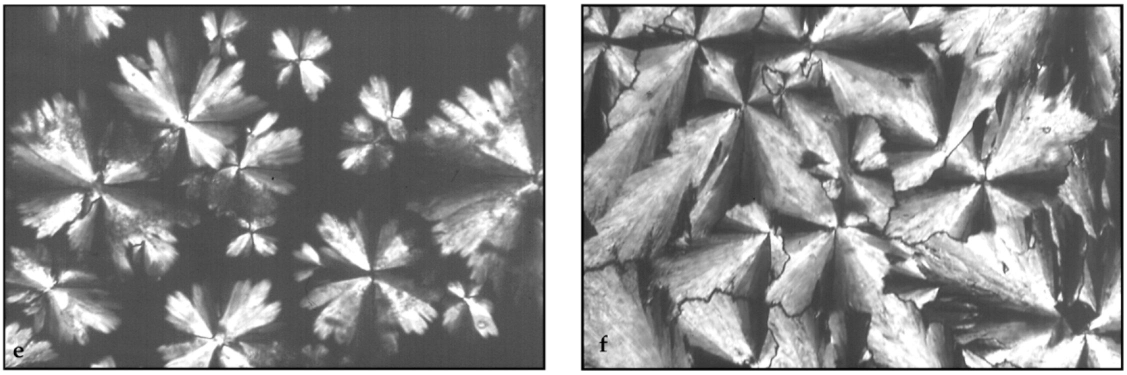

Fig. 5. (*continued*)

was too thin to span the gap between the cover slips. When thick enough to adhere to both surfaces and fail cohesively when the slips were separated, the individual lamellae can be seen (Fig. 5b). With the T_m of 180°C/72 h bulk polymerized DMT/PDO samples being 180°C, the growth of spherulites in the melt at 195°C is unexpected. The structures in the TEM micrographs could have formed during cooling, but those in Fig. 5 are formed at the polymerization temperature, one that is expected to be well above the T_m of the initially forming polymer. As suggested by the DSC results, the chains may grow until the crystallization temperature reaches the polymerization temperature following which the polymer precipitates out of solution (melt).

In thinner portions of the films for the 210°C T_p samples, lamellar single crystals, with ca. 85 Å thickness were formed with both TCl and DMT (Fig. 7a–c). The TCl/PDO crystals are similar in appearance to those of DMT/PDO polymerized at lower temperature (e.g. Fig. 2b), consisting of ribbons organized into fronds, whereas those of DMT/PDO are relatively broad. In addition, The TCl/PDO 180°C/24 h crystals resemble the PBT TCl/BDO 190°C/8 h crystals (Fig. 1, Ref. [3]) in having well-defined lamellae, while the TCl/PDO 210°C/20 h crystals resemble the PBT TCl/BDO 210°C/20 h crystals (Fig. 2, Ref. [3]), consisting of radial aggregates of “frond-like” crystals. Thus, for each set of monomers, for PET, PBT and PTT, there seems to be an optimum range of temperature to grow “nice” lamellar single crystals.

At 220°C/14 h TCl/PDO yielded a considerably different morphology (Fig. 8a). The crystals are thick, elongated structures resembling those found for PET polymerized by CTFMP at 225°C (Figs. 2d and 3, Ref. [2]; lower T_p for PET, as for PTT, yielded lamellar crystals). Although there is some suggestion, as also for PET, that these thick crystals consist of lamellae at an angle to the substrate, their morphology is not clear. As for the lamellar crystals lying on the substrate, these crystals also give $[20\bar{1}]$ ED patterns. DMT/PDO, however, even for long t_p still yielded thin, lamellar crystals (Fig. 8b).

Totally unexpected was the morphology of the crystals formed at 220°C from TCl/PDO, with and without an N_2 atmosphere, for long t_p (Fig. 9a and b). After 48 h thick, smooth crystals were found, often growing out from the substrate. After 60 h, the growth out from the substrate was emphasized further, the crystals appearing as, we believe, four-sided needles protruding out from the substrate. As shown by the insets, thin striations can be observed on their sides, suggesting they consist of stacks of lamellae, possibly growing as a single crystal whisker. The considerable difference in morphology and the long t_p at high T_p suggests the possibility that they are degradation products, but the ED patterns are appropriate for PTT. In addition, we have recently seen similar structures formed during the polymerization of poly(heptamethylene terephthalate) by CTFMP from TCl and heptanediacetate at

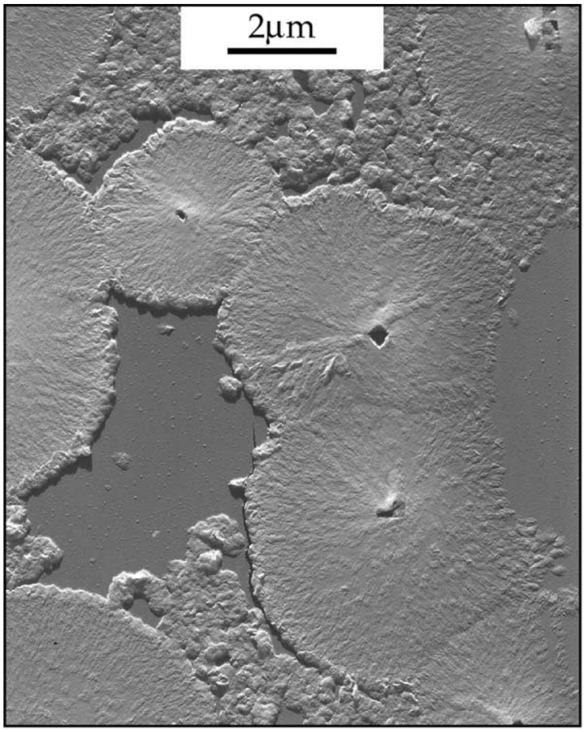

Fig. 6. Spherulites in a thin CTFMP film of TCl/PDO, 210°C/7 h, grown between glass.

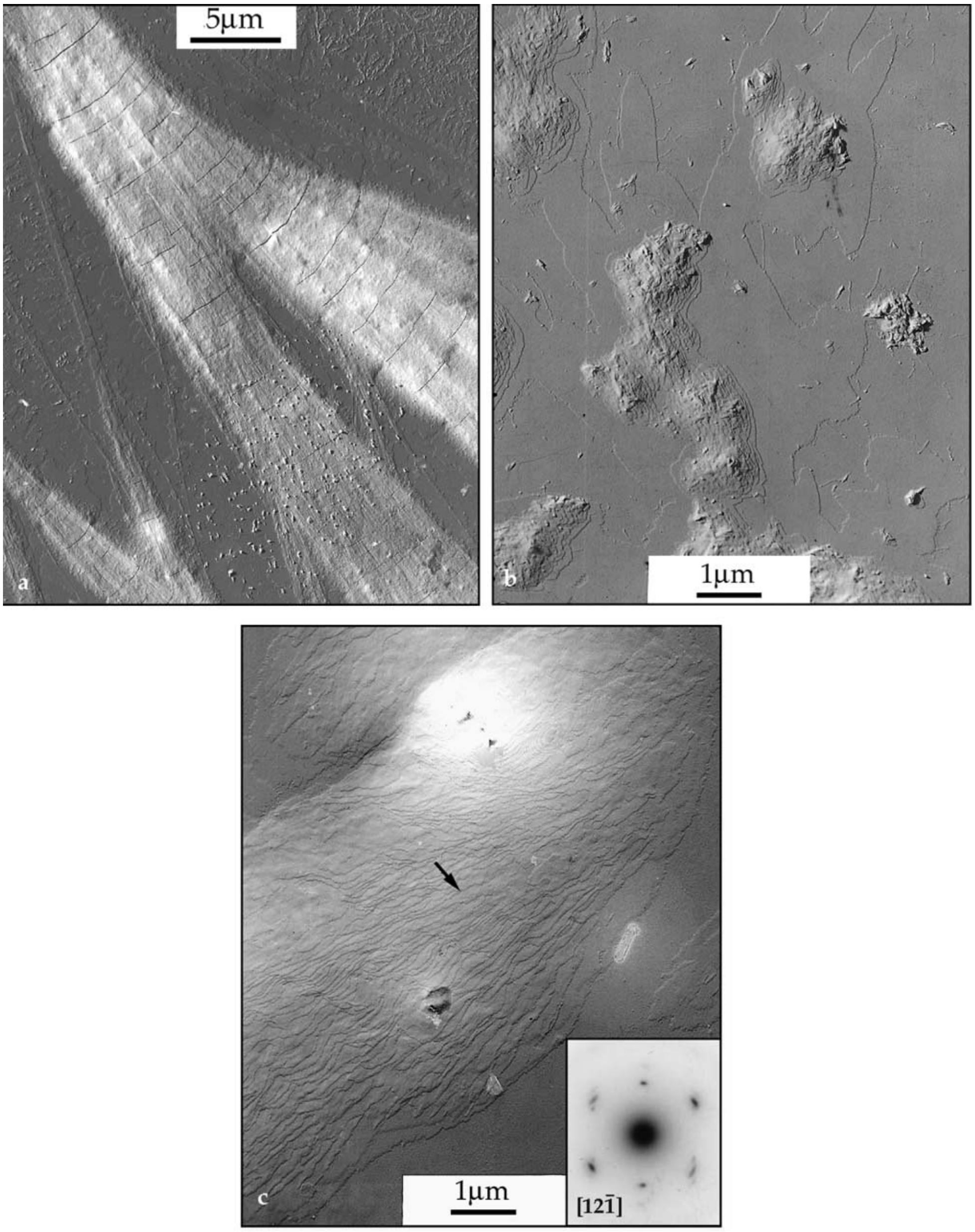

Fig. 7. CTFMP samples of: (a) TCl/PDO, 210°C/20 h between glass; (b) DMT/PDO, 210°C/24 h, between glass with N_2 atmosphere and (c) DMT/PDO, 210/20 h on mica. Epitaxy of PTT on mica was not found for any conditions.

180°C/24 h and poly(nonamethylene terephthalate) from TCl and both nonanediacetate (200°C/48 h) and nonanediol (180°C/24 h) [14].

3.2. Characterization

Of concern in all of our relatively low T_p polymerizations is whether we have actually formed the desired polymer. Figs. 10–13 are DSC, FTIR, WAXD and SAXD scans, respectively, of a commercial PTT (supplied by Dr B. Hsaio, DuPont), and several DMT/PDO samples polymerized in the bulk in a test tube at 180, 200 and 220°C for (in most figures), 72 h. Because of the low boiling point of PDO, several DMT/PDO ratios were used. No significant difference was seen for the results with PDO concentration; for the samples in the figures a 1/3 ratio was used for the 180 and 220°C T_p samples and a 1/6 ratio for the 200°C T_p sample.

The DSC scans (Fig. 10) indicate a lower T_m, ca. 180 for all polymerization temperatures, than for the solution precipitated DuPont PTT; the DuPont material is also seen to have a double peak as does the 220°C/72 h sample. During cooling, all three T_p samples crystallized 10–20°C below the DuPont sample, with the 200°C T_p sample having the highest T_m and T_c. On a second heating, the main T_m of the three T_p samples increased to near 200°C, each having a second peak ca. 20°C lower in T. On the other hand, the T_m of the

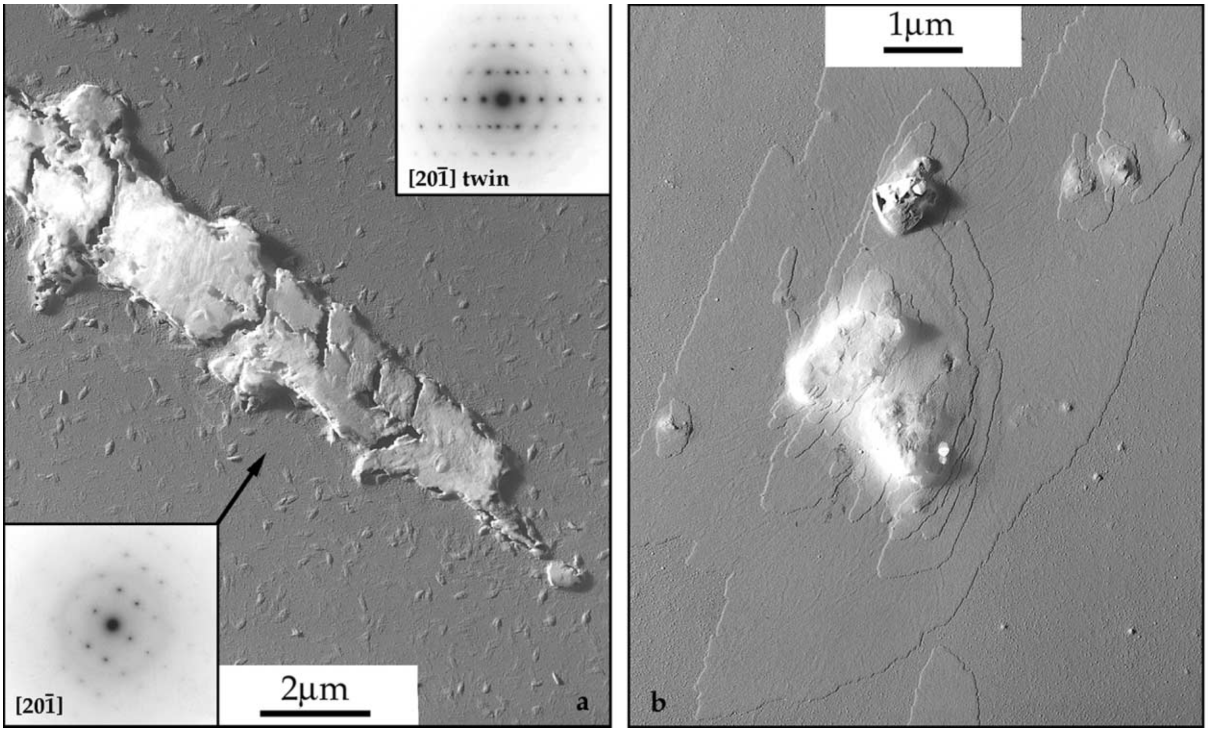

Fig. 8. (a) CTFMP sample of: TCl/PDO, 220°C/14 h, between glass and (b) DMT/PDO, 220°C/60 h between glass with N_2 atmosphere.

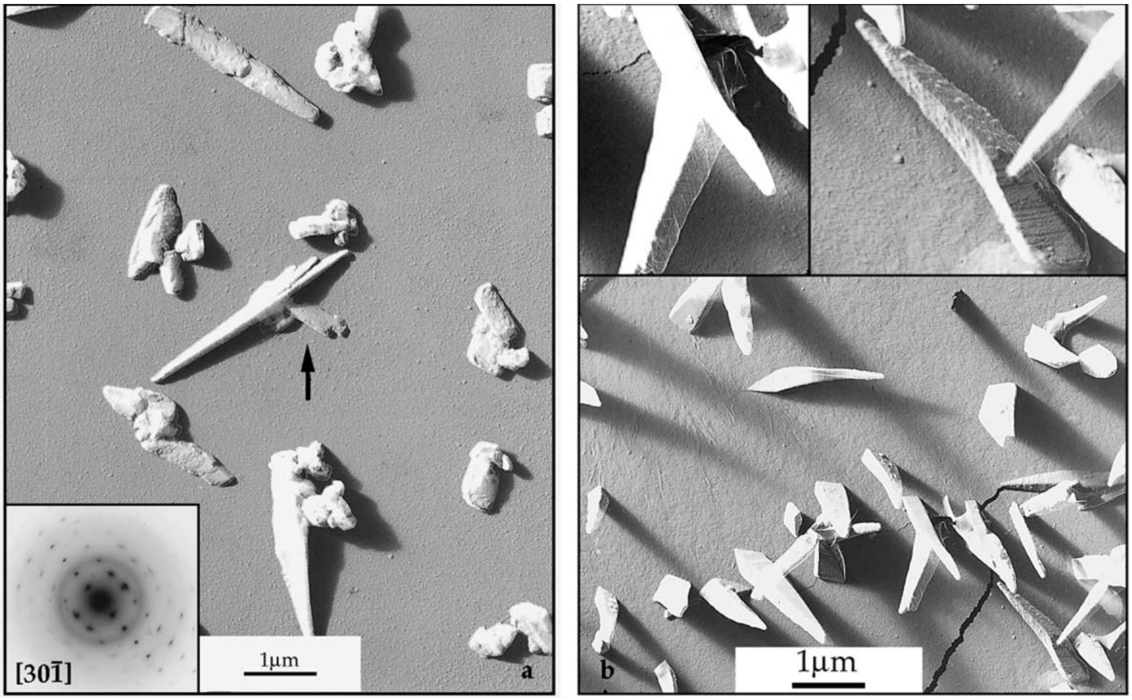

Fig. 9. CTFMP samples of DMT/PDO polymerized at 220°C for: (a) 48 h and (b) 60 h. The ED pattern inset in (a) is from the area indicated by the arrow; insets in (b) are higher magnifications of two of the needles.

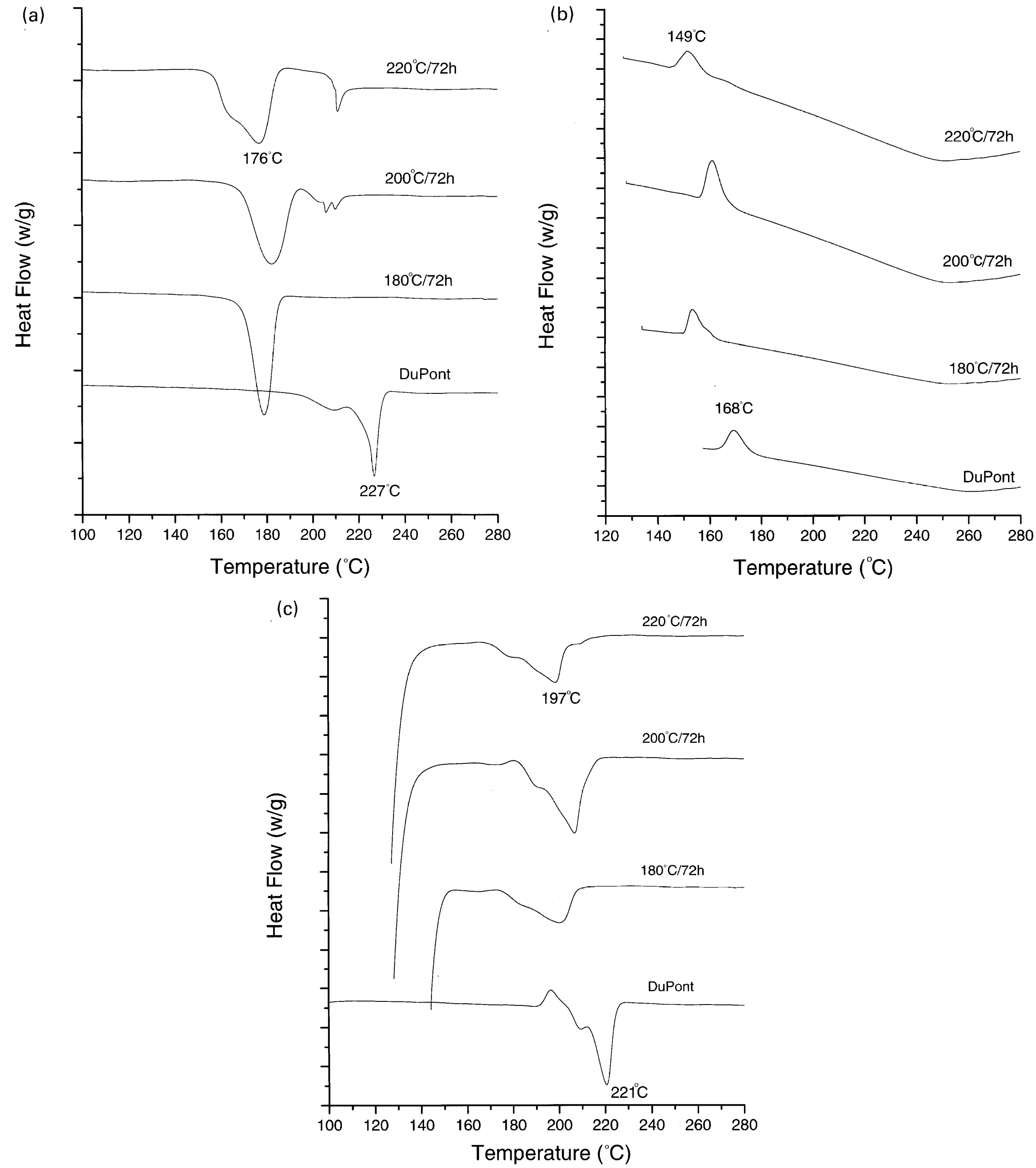

Fig. 10. DSC scans of the solution precipitated DuPont PTT and several bulk polymerized DMT/PDO samples. Heating rate is 20°C/min: (a) first heating; (b) first cooling, and (c) second heating.

DuPont sample decreased. Several of the samples on second heating have an apparent exothermic peak just below the endothermic peaks; this may be due to crystallization of material not crystallized during cooling. However, it is considerably further above T_g than in the case of, for instance, PET which undergoes cold crystallization at 110°C, 45°C above T_g. On first heating, the 200 and 220°C T_p samples have several small endothermic peaks above T_m, approximately at the same position as the much larger melting peaks on second heating. We attribute them to small amounts of high molecular weight material formed on first heating, with the higher T_m on second heating due to chain extension on the first heating to 280°C. Melting points and heats of fusion and crystallization of all the samples are given in Table 1. On first heating, ΔH_f was larger for the as-polymerized samples, regardless of T_p, t_p or DMT/PDO ratio, than for the DuPont sample, in agreement with the higher crystallinity we normally find for as-polymerized polymers than after any subsequent thermal processing. This is even though the DuPont PTT had been precipitated from solution. During cooling and reheating the enthalpy changes are smaller, with the DuPont sample now having the larger values.

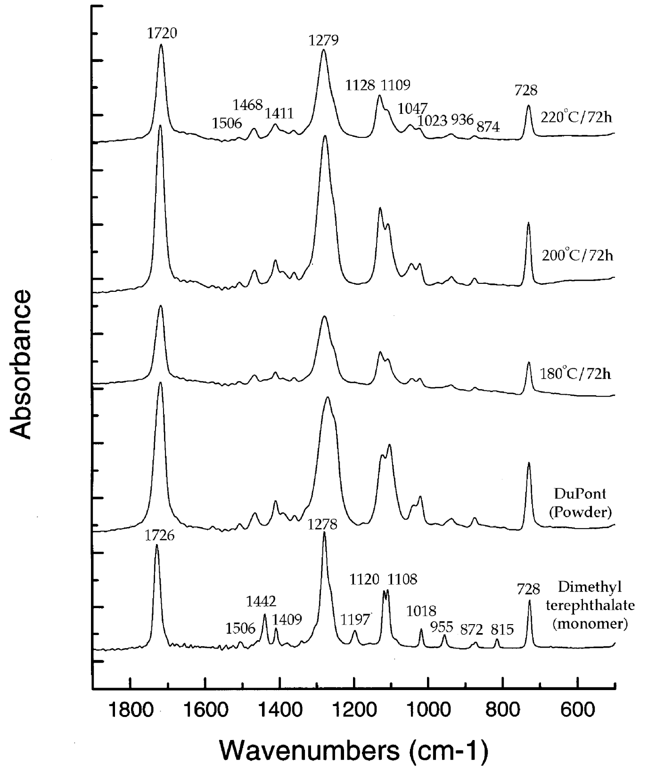

Fig. 11. FTIR scans of DMT, the solution precipitated DuPont PTT and several bulk polymerized DMT/PDO samples.

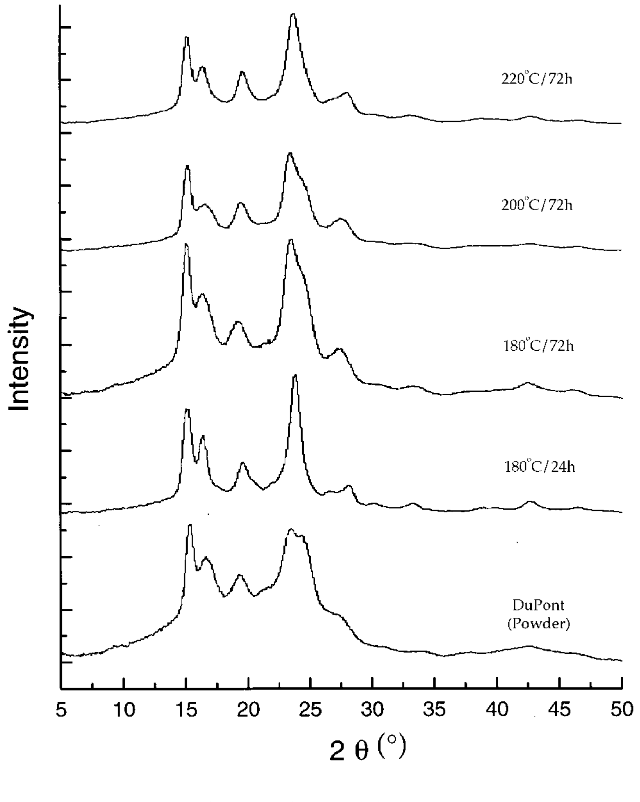

Fig. 12. WAXD scans of the solution precipitated DuPont PTT and several bulk polymerized DMT/PDO samples. A scan of a 180°C/24 h sample is shown in addition to the scans of the samples in Figs. 10, 11 and 13.

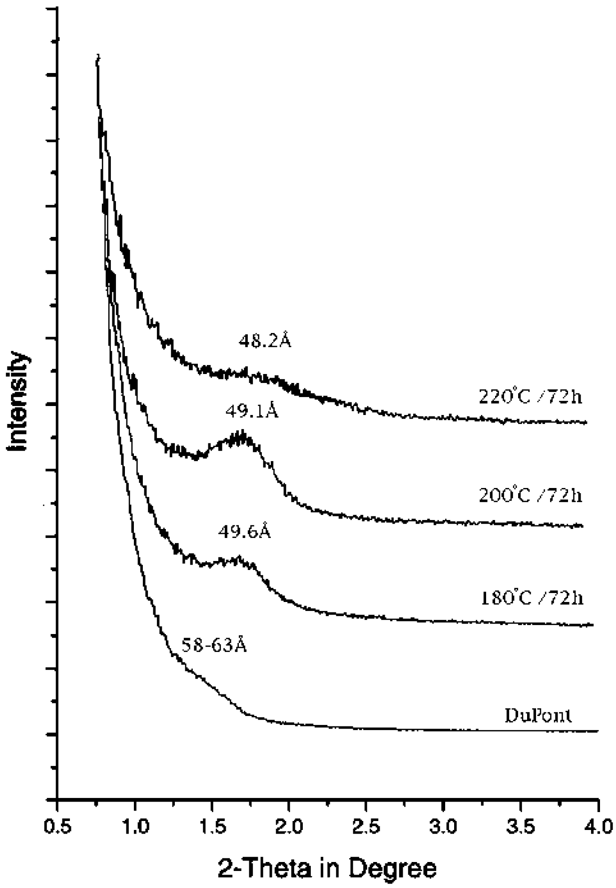

Fig. 13. SAXD scans of DuPont PTT and several bulk polymerized DMT/PDO samples.

The FTIR scans (Fig. 11) are also similar, the main difference being the relative height of the two split peaks in the 1100–1300 cm^{-1} wavenumber region. The split peaks at ca. 1115 cm^{-1} are attributed to the C–O aliphatic carbon ester bond, those at ca. 1270 cm^{-1} (1279 cm^{-1} and its shoulder) to the C–O carbonyl carbon ester bond. As shown in Ref. [15], for PET, these bands are each triplets for "pure amorphous" PET (with peak heights $1100 > 1119 > 1138\ \mathrm{cm}^{-1}$ and $1264 > 1246 > 1286\ \mathrm{cm}^{-1}$) while they are doublets in "pure crystalline" PET ($1130 > 1112\ \mathrm{cm}^{-1}$ and $1255 \geqq 1274\ \mathrm{cm}^{-1}$). In our samples, there are contributions from both the crystalline and amorphous bands, the bands presumably overlapping. We attribute the change in relative heights of the 1109–1128 cm^{-1} to the higher crystallinity of the as-polymerized material. The intensity of the band at ca. 1279 cm^{-1} is always greater than that at about 1255 cm^{-1}, presumably because of the use of PTT instead of PET. The splitting of both sets of peaks is smaller in the DMT monomer, presumably due to the aliphatic carbon being part of a methyl rather than propyl group.

WAXD scans (Fig. 12) indicate that the bulk of as-polymerized material is both of higher crystallinity and with more perfect (as shown by the larger number of resolvable reflections) than the DuPont solution precipitated

Table 1
The T_m and H_m, H_c and SAXD periodicity of PTT DMT/TMD bulk samples

Sample	First heating[a]		Second heating		First cooling		SAXD
	T_m (°C)	H_m (J/g)	T_m (°C)	H_m (J/g)	T_c (°C)	H_c (J/g)	(Å)
DuPont[b]	227/209	91	221/209	71	168	67	60
180°C/72 h, 1:3	180	115	202/185	–	153	71	50
180°C/72 h, 1:6	179	111	200/183	59	152/157/163	79	50
200°C/72 h, 1:3	180/207	98/7.6	205	70	152/157/162	99	49
200°C/72 h, 1:6	182/206/210	68/10.3	207 (190?)	64	161.3	73	53
210°C/24 h, 1:6	151/202/248	–	198	52	149.39	74	46
220°C/72 h, 1:3	177/211	100/8.5	198	45	152.0	54	48
220°C/72 h, 1:6	166/176/212	1138/3.2	197	53	153.2	78	48

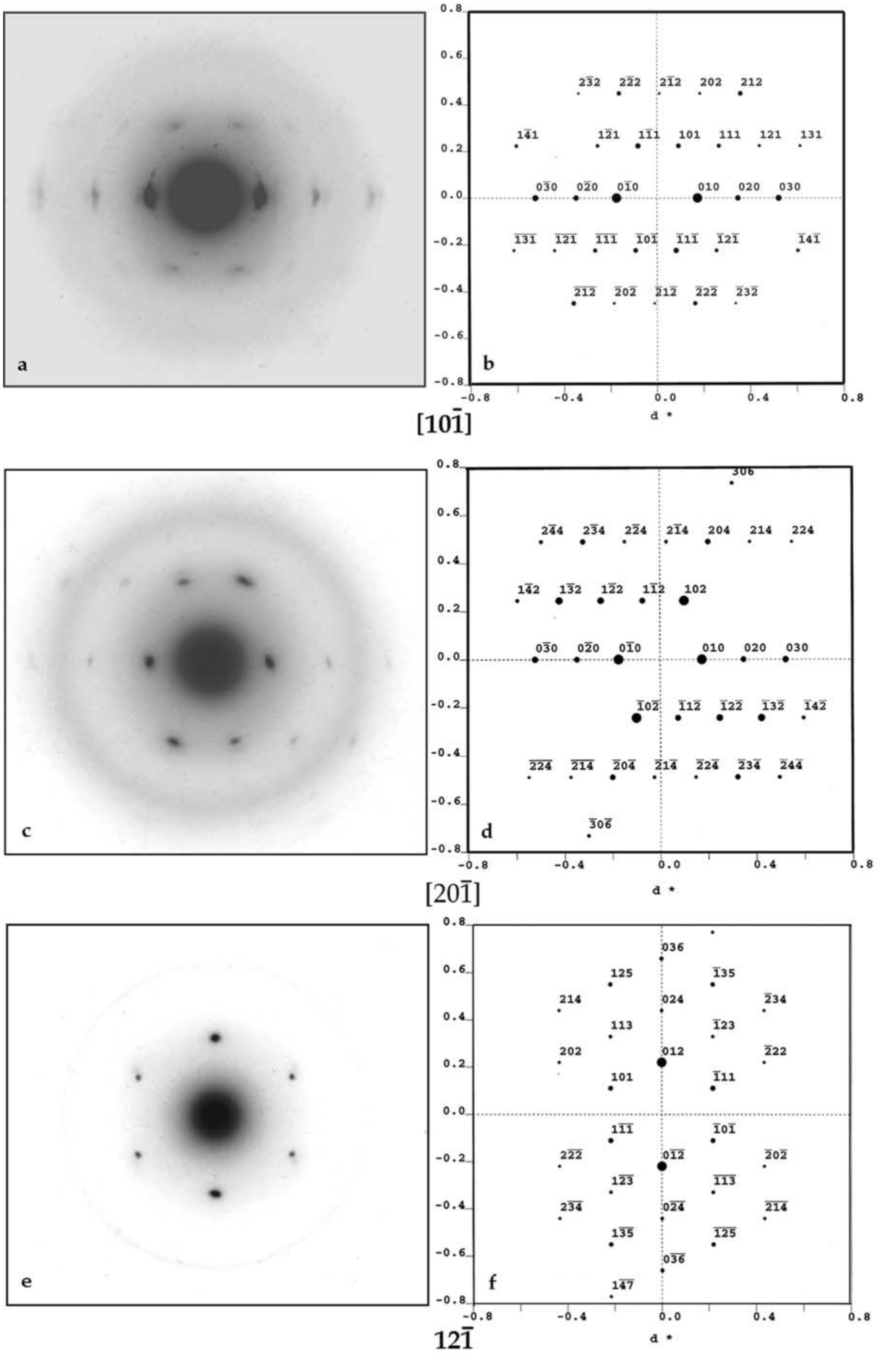

Fig. 14. ED patterns from various CTFMP samples; most correspond to the inset patterns on previous figures. The corresponding Cerius[2] simulations are shown except for (j) which is a [001] pattern simulation.

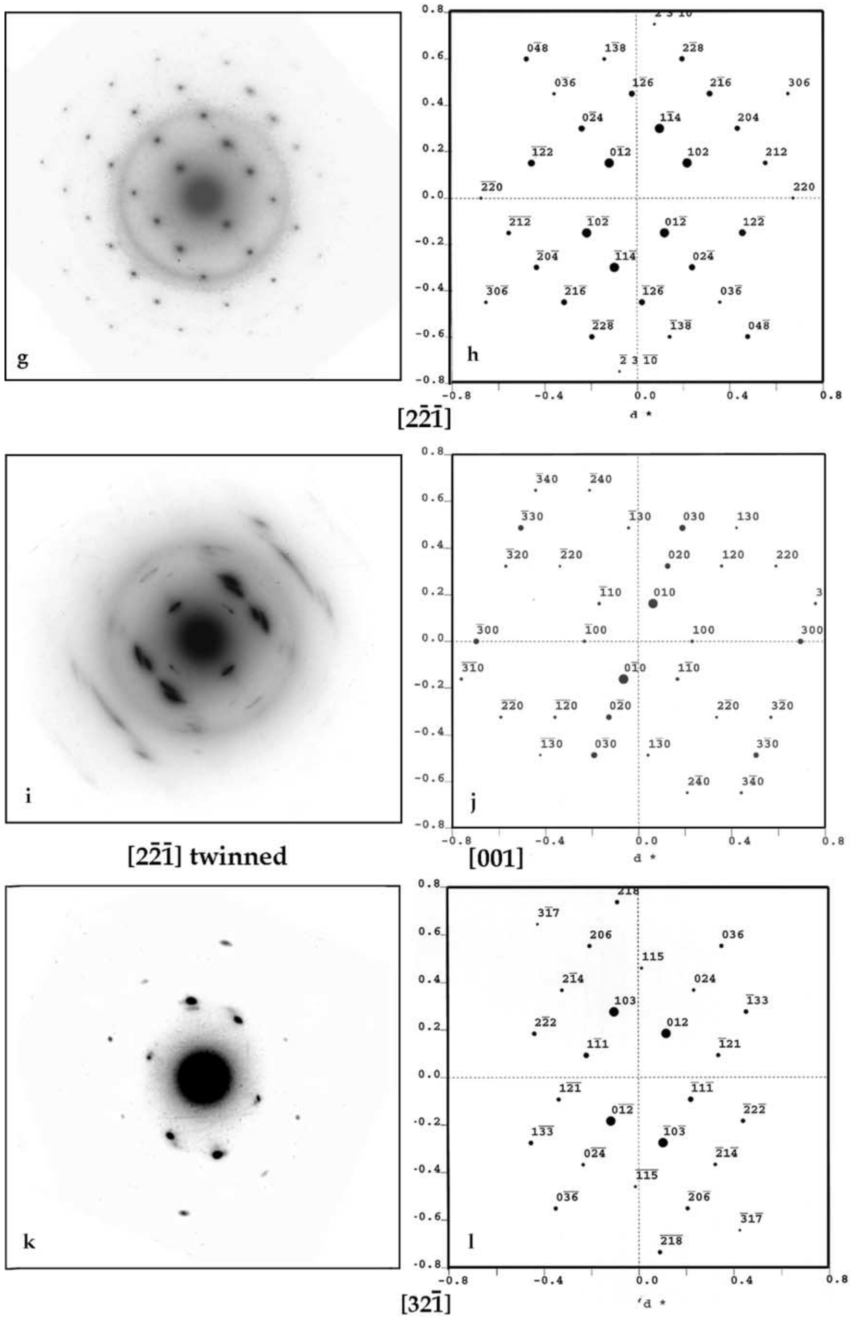

Fig. 14. (*continued*)

material, in agreement with the DSC results. Only the peak positions of the 180°C/24 h sample differs slightly in that the peak at 23.7° 2θ lies between the 23.5° peak and its shoulder in the other samples and the peak at 27.5° is split into peaks at 26.4 and 28.2°. This may be due to a relatively low molecular weight. SAXD scans (Fig. 13) of the bulk of as-polymerized material have peaks at about 50 Å; values for all samples are listed in Table 1. Whether this is first- or second-order could not be determined because of the high diffuse scatter at smaller angles; based on the CTFMP samples, all of which have lamellar thicknesses of ca. 100 Å, we suggest that it is second-order. Despite the similarity of the thicknesses of the CTFMP crystals, one might have expected the higher T_p samples to have larger thicknesses, the oligomers polymerizing until the crystal thickness of the extended chain crystals equals the crystallization temperature of the growing liquid crystals. The commonality of the DSC, SAXD and IR results suggests a T_p independent crystal thickness and degree of polymerization. This is similar to the results obtained for CTFMP preparations for all of the polymers we have prepared; the lamellar thickness of the resulting lamellae is generally

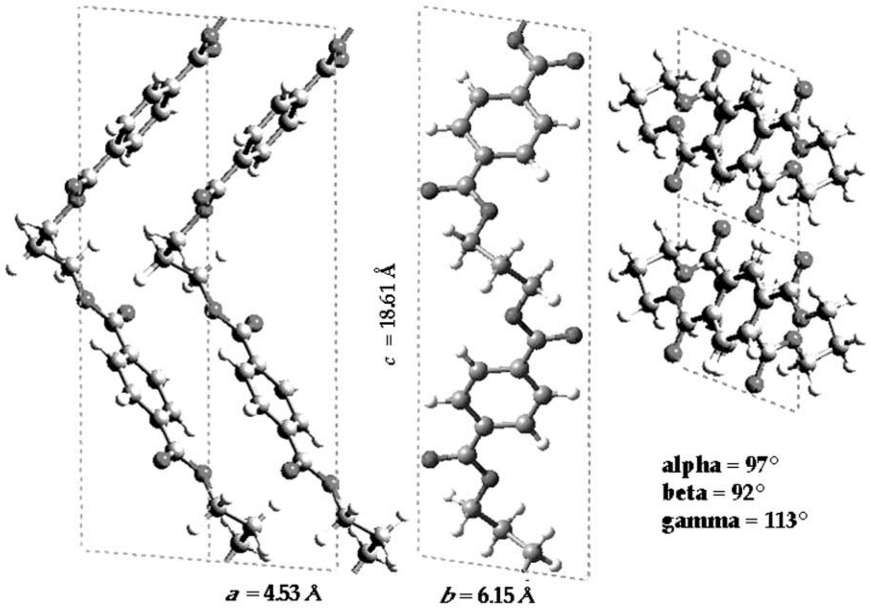

Fig. 15. Proposed PTT unit cell based on the ED patterns.

ca. 100 Å regardless of the T_p and t_p. Reheated samples, e.g. from the DSC first heating experiments, were not examined by either WAXD or SAXD. The DuPont material has only the suggestion of a SAXD peak at slightly smaller angles, again on a high diffuse scattering background.

3.3. Electron diffraction and crystal structure

Contrary to nearly all other CTFMP polymers we have examined, [001] ED patterns were not obtained. The most common was [$20\bar{1}$] with the other observed patterns retaining the $l = \bar{1}$ index. Wang et al., in a paper also published in this issue, [8] took a series of ED patterns from PTT melt grown single crystals while rotating about the b^* axis, obtaining [$h0\bar{1}$] and [$h01$] patterns, with $h = 1$–4. Their patterns are consistent with ours. Their [001] pattern has only $0k0$ reflections. As shown below, this is due to the fact that all $l = 0$ index reflections, except 010, are extremely weak. Typical ED patterns we obtained are shown in Fig. 14, along with CERIUS^2 simulations based on the unit cell we propose shown in Fig. 15. Two cells are shown for the [010] and [001] projection to show the relative positions of the molecules. Unit cell parameters are listed in Table 2 for literature data and our data as obtained from the DuPont fiber (as a fiber) and bulk polymerized material (180°C/72 h) by X-ray diffraction and the ED patterns from the CTFMP samples. Most of the literature data was obtained from X-ray fiber patterns; Poulin-Dandurand et al. [11] also obtained [001] ED patterns from solution grown single crystals. Wang et al. [8] used ED patterns from melt-crystallized lamellar crystals to index and refine an X-ray powder pattern from a sample isothermally crystallized from the melt at 150°C. As for PET [2], we attribute at least some of the variation in unit cell parameters and density to variations in processing history, with the CTFMP samples having the highest density ("most perfect crystal") and the

Table 2
Unit cell data for polytrimethylene terephthalate

	a (Å)	b(Å)	c (Å)	α (°)	β (°)	γ (°)	ρ (g/cm^3)
Poulin-Dandurand et al. [11]	4.637	6.266	18.64 (fiber axis)	98.4	93.0	111.1	1.387
Desborough et al. [16]	4.620	6.200	18.30	98.0	90.0	112.0	1.427
Tadokoro [17]	4.58	6.22	18.12	96.9	89.4	111.0	1.43
Hall [7] (best estimates)	4.60 ± 0.03	6.22 ± 0.01	18.36 ± 0.25	97.8 ± 0.6	90.8 ± 1.9	111.3 ± 0.4	1.414(unit cell) 1.35(measured)
Wang et al. [8] melt crystallized (WAXD)	4.6(3)	6.1(2)	18.6(1)	97.5	92.1	110	1.40
DuPont-fiber (WAXD)	4.42	6.23	18.75	98.13	91.24	112.09	1.406
Bulk (180°C/72 h) polymerized (WAXD)	4.57	6.41	18.65	98.57	91.45	112.20	1.431
ED (TEM)	4.53	6.15	18.61	96.87	92.21	110.97	1.448

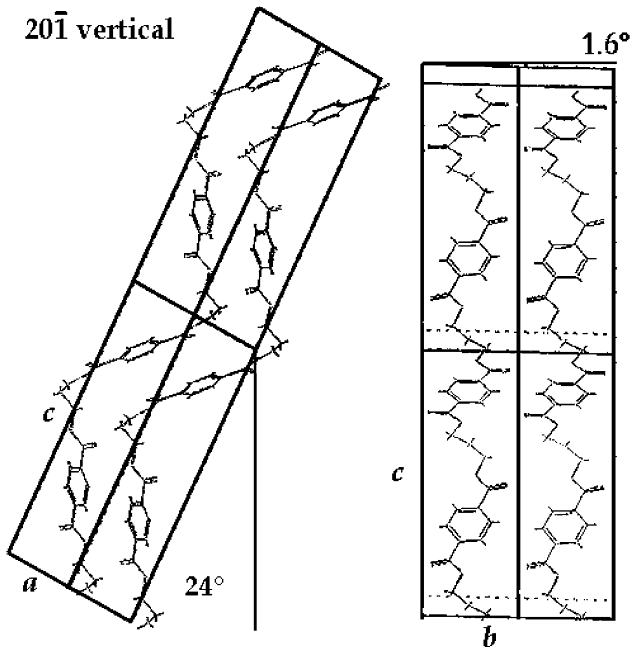

Fig. 16. [010] and [100] projections of the unit cell with $[20\bar{1}]$ vertical, i.e. parallel to the electron beam in the TEM so as to give a $[20\bar{1}]$ ED pattern.

as-polymerized bulk sample the next highest. Our fiber pattern is seen to have a larger value of *c* and a smaller value of *a*, corresponding to extending the zig-zag.

The simulated ED patterns are also shown in Fig. 14, with a simulated [001] pattern in Fig. 14j. The relative intensities of the patterns and the simulations are in good agreement, as are the X-ray patterns and its CERIUS^2 simulation (not shown). As indicated by the [001] projection of the unit cell in Fig. 15, an electron density periodicity is seen most clearly along b^*; the lack of a periodicity in the other directions; the large zig-zag of the molecule and the overlap of adjacent molecules along *a* results in weak periodicities and thus a lack of reflections. The origin of the predominance of $[20\bar{1}]$ ED patterns from both CTFMP grown single crystals is not clear. As shown in Fig. 16, when $[20\bar{1}]$ is vertical, one of the PTT residues is also nearly vertical, but the ends of the CTFMP molecules, for instance, would not all lie on the substrate along *a*. The latter would be expected for extended chain CTFMP crystals with high interaction between the monomer and substrate; the presence of the latter is shown by the need to dissolve the substrate with HF to remove the crystals. Along *b* the ends are nearly aligned with the substrate with $[20\bar{1}]$ vertical. With b^* being parallel to the long axis of some of the crystals (Figs. 3, 7c and 8a) but perpendicular in others (Fig. 2b) we cannot correlate the shape of the unit cell with the morphology.

4. Conclusions

1. As for PET and PBT, extended chain, lamellar, single crystals ca. 100 Å thick can be grown by the CTFMP method in thin films using either TCl or DMT as comonomer with PDO, at temperatures both above and below the T_m (225°C) of high MW PTT. For all three polymers growth at ca. 180–200°C leads to well developed lamellar crystals, with more complex structures developing for higher and lower T_p. Polymerization in thicker films leads to the growth (at 195°C) of lamellar spherulites which appear to grow simultaneously with polymerization. Bulk polymerization at 180–220°C, using DMT/PDO, also yields lamellar material; SAXS indicates ca. 50 Å spacing (second-order?), with a first melting peak at ca. 180°C T_m regardless of the T_p.
2. Refinement of the triclinic unit cell, using spacings from the ED patterns leads to the following parameters: $a = 4.53$ (4.63, 4.60; values of Wang et al. this symposium [8] and Hall [7]), $b = 6.15$ (6.12, 6.22), $c = 18.61$Å (18.61, 18.36), $\alpha = 97°$ (97.5, 97.8), $\beta = 92°$ (92.1, 90.8), $\gamma = 111°$ (110, 111.3), $\rho = 1.448$ g/cm^3 (1.398, 1.414). Modeling using CERIUS^2 indicated a single segment cell (shown in Fig. 15) resulted in simulated ED patterns that matched the observed patterns well; *R* was not determined.
3. Intermediate to PET and PBT, the "perfect" crystal has a slightly more dense unit cell than processed (fibers) material; *c* is slightly shorter and *a* and *ρ* larger. Bulk polymerized material is intermediate. For PET, there is a significant difference in crystal density with processing history whereas for PBT the crystal density of CTFMP material and fibers is approximately the same [2,3].
4. A problem remains with the relationship between the most frequent $[20\bar{1}]$ ED patterns from the lamellae and the molecular orientation. From past experience, we expect the carboxyl end groups to attach to the substrate; if molecular tilt along *a* is expected but not to the extent required for $[20\bar{1}]$ to be parallel to the electron beam.

Acknowledgements

This research was supported, in part, by the National Science Foundation, Polymers Program, through grants 93-12823 and 96-16255.

References

[1] D'Aquino RL. Three routes vie for the 1,3-propanediol market. Chem Engng 1999;106:56.

[2] Liu J, Geil PH. Crystal structure and morphology of poly(ethylene terephthalate) single crystals prepared by melt polymerization. J Macromol Sci, Phys B 1997;36(1):61–85.

[3] Liu J, Geil PH. Electron diffraction and computer modeling studies of the crystal structure of poly(butylene terephthalate) a-form single crystals. J Macromol Sci, Phys B 1997;36(2):263–80.

[4] Liu J, Sidoti G, Hommema JA, Geil PH, Kim JC, Cakmak M. Crystal structure and morphology of thin film, melt crystallized poly(ethylene naphthalate). J Macromol Sci, Phys B 1998;37(4):567–86.

[5] Rybnikar F, Liu J, Geil PH. Thin film melt polymerized single crystals of poly(*p*-oxybenozate). Macromol Chem Phys 1994;195:81–104.

[6] Product of Molecular Simulations, Inc., San Diego, CA.

[7] Hall IH. The determination of the structures of aromatic polyesters from their wide-angle X-ray diffraction patterns. In: Hall IH, editor. Structure of crystalline polymers. London: Elsevier Applied Science, 1984. p. 39–78.

[8] Wang B, Li CY, Cheng SZD, Geil PH, Grebowicz J, Ho R-M. Poly(trimethylene terephthalate) crystal structure and morphology in different length scales. Polymer 2001;42:7171.

[9] Mencik Z. Krystalická struktura polykondenzátu kyseliny naftalen-2,6-dikarbonové s etylénglykolem. Chem Prum 1967;17:78–81.

[10] Cakmak M, Kim JC. Structure development in high-speed spinning of polyethylene naphthalate (PEN) fibers. J Appl Polym Sci 1997; 64(4):729–48.

[11] Poulin-Dandurand S, Perez S, Revol J-F, Brisse F. The crystal structure of poly(trimethylene terephthalate) by X-ray and electron diffraction. Polymer 1979;20(4):419–26.

[12] Liu J, Long T-C, Geil PH, Rybnikar F. Poly (terephthalic anhydride) single crystals: morphology and crystal structure. J Polym Sci, Polym Phys B 1996;34(17):2843–51.

[13] Program supplied by Zhang A, Department of Polymer Science, University of Akron, Akron, OH.

[14] Yang J. Unpublished results.

[15] Cole KC, Guevremont J, Ajji A, Dumoulin MM. Characterization of surface orientation in poly(ethylene terephthalate) by front-surface reflection infrared spectroscopy. Appl Spectrosc 1994;48(12):1513–21.

[16] Desborough IJ, Hall IH, Neisser JZ. The structure of poly(trimethylene terephthalate). Polymer 1979;20(5):545–52.

[17] Tadokoro H. Structure of crystalline polymers. New York: Wiley–Interscience, 1979. 369 p.